

Fabrication of metal nanoparticle arrays by controlled decomposition of polymer particles

D Brodoceanu¹, C Fang², N H Voelcker³, C T Bauer¹, A Wonn¹, E Kroner¹, E Arzt¹ and T Kraus¹

¹ INM-Leibniz Institute for New Materials, Campus D2 2, 66123, Germany,

² School of Chemical and Physical Sciences, Flinders University, Bedford Park, SA 5042, Australia,

³ Mawson Institute, University of South Australia, Adelaide, SA 5001, Australia

E-mails: daniel.brodoceanu@inm-gmbh.de, tobias.kraus@inm-gmbh.de

Abstract

We report a novel fabrication method for ordered arrays of metal nanoparticles that exploits the uniform arrangement of polymer beads deposited as close-packed monolayers. In contrast to colloidal lithography that applies particles as masks, we use thermal decomposition of the metal-covered particles to precisely define metal structures. Large arrays of noble metal (Au, Ag, Pt) nanoparticles were produced in a three-step process on silicon, fused silica and sapphire substrates, demonstrating the generality of this approach. Polystyrene spheres with diameters ranging between 110 nm and 1 μ m were convectively assembled into crystalline monolayers, coated with metal and annealed in a resistive furnace or using an ethanol flame. The thermal decomposition of the polymer microspheres converted the metal layer into particles arranged in hexagonal arrays that preserved the order of the original monolayer. Both particle size and interparticle distance were adjusted via thickness of the metal coating and sphere diameter, respectively.

1. Introduction

Interest in developing fabrication methods for metal nanoparticle (NP) arrays is spurred by their wide spectrum of applications that include surface-enhanced Raman spectroscopy,^[1] light-trapping applications in solar cells,^[2-4] templates for 3D surface nanostructuring,^[5] surface biofunctionalization,^[6] sensors,^[7] catalytic surfaces^[8] and surface plasmon resonance.^[9] Research focuses on capabilities for patterning large areas with a minimum number of processing steps. In this regard, one attractive

alternative to conventional methods is colloidal lithography.^[10-13] Here, the long-range order of self-assembled polymer monolayers is transferred into an underlying substrate through subsequent processes (e.g. shadowed evaporation, reactive-ion etching,^[14-19] electrochemical etching,^[20] vapour-liquid-solid growth (VLS),^[21] metal assisted etching).^[22] The resulting NP arrays have either one or two particles per unit cell,^[23] where the former is usually more challenging and demands more processing steps.

One efficient route to metal NP arrays uses core-shell particles which consist of a core metal NP surrounded by a polymer shell.^[24, 25] They can be deposited as close-packed monolayers by convective assembly on virtually any smooth surface. Their shells are then thermally decomposed or plasma etched, leaving the metal NP cores in a regular hexagonal array. The maximum diameter of core-shell particles that decompose into compact nanoparticles (NPs) rather than granular structures is currently 260 nm,^[26] which restricts the maximum spacing accessible with this route. Furthermore, regular arrays require monodisperse particles with minimum deviations from the spherical shape, conditions which are difficult to achieve with the current core-shell syntheses. Here, we follow the inverse strategy and create metal shell – polymer core particles. We deposit polymer particle monolayers by convective assembly and coat them with metal shells using physical vapour deposition (Figure 1).

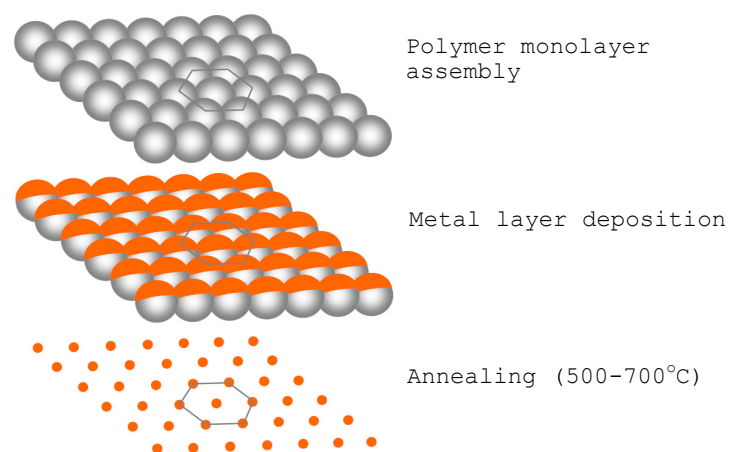


Figure 1. Schematic representation of our three-step process. A polystyrene monolayer is assembled on a substrate. A noble metal layer is deposited. Thermal annealing is finally performed either in a resistive furnace or using an ethanol flame, resulting in an array of metal nanoparticles.

Thermal decomposition removes the polymer cores, sinters the metal layers and yields metal particle arrays with excellent long-range order. We demonstrate the effectiveness of this method for generating

arrays of noble-metal particles with size ranging from 50 nm to 400 nm using polystyrene (PS) microspheres with diameters between 110 nm and 1 μm on flat and curved substrate surfaces.

In conventional colloidal lithography, a metal is deposited in the spheres' interstices which yields the non-close-packed patterns illustrated in Figure S1a (Supplementary data). Such patterns can be annealed to convert the ordered, quasi-triangular islands into rounded metal NPs.^[27, 28] Our approach allows us to pattern dense metal arrays with tuneable particle size and spacing in fewer steps (Fig. S1b). Furthermore, the entire metal is converted into particles, unlike in conventional lithography, where a significant fraction is lost in the process.

2. Fabrication and experimental details

All chemicals were obtained from commercial sources and used without further purification. We used commercial colloidal suspension of monodisperse polystyrene microspheres with mean diameters of 110 nm (Invitrogen, Germany), 250 nm (BangsLabs, USA), 520 nm (BangsLabs, USA), 1 μm (Invitrogen, Germany), 3 μm (Invitrogen, Germany) and 15 μm (Invitrogen, Germany).

The three-step process is schematically depicted in Fig.1.

Step 1: Fabrication starts with close-packed monolayers that we deposited by convective assembly over approximately one square centimetre of silicon, fused silica or sapphire surface. The substrates were cleaned in an ultrasonic bath using isopropanol (Sigma-Aldrich, Deisenhofen, Germany, puriss. p.a.), rinsed with deionised water (Millipore unit) and dried under a nitrogen stream. Before monolayer deposition, the substrates were treated in oxygen plasma for 5 min at 0.3 mbar (low-pressure reactor PICO, RF source at 13.56 MHz, Diener electronic, Ebhausen, Germany) at 50 W RF power to remove contaminants and render their surfaces hydrophilic. Compact monolayers were deposited using a convective assisted particle assembly setup described elsewhere.^[29-31] Alternatively, a dip-coating technique was employed to deposit a monolayer of polystyrene spheres on the outer wall of a glass tube with diameter of 180 μm .

Step 2: The monolayers were coated with 5 nm - 70 nm of a noble metal (Au, Ag or Pt) using a standard magnetron sputter-deposition system (Autofine Coater, JEOL JFC-1300, Japan) at normal (0°) or at oblique incidence (45° - 70° , angle between the sputtering beam direction and substrate normal).

The deposition was performed in argon at 0.08 mbar and a discharge current of 40 mA, while the distance between samples and metal target was 5 cm.

Step3: The metal-coated polymer spheres were annealed at temperatures in the range of 500-700 °C in air for up to 60 min using a resistive furnace (NABERTHERM, Germany). Alternatively, the samples were exposed to an ethanol flame for up to 2 min, where a simple burner ensured a stable flame. Finally, some samples were etched in an aqueous solution of 0.33 g/l I₂ and 0.67 g/l KI for between 2 and 10 min.

The fraction area occupied by the particles with respect to the bare substrate surface was estimated using ImageJ software and represents the percentage of pixels in the SEM image that have been highlighted using Image/Adjust/Threshold.

For the metal-assisted chemical etching experiment, the gold nanoparticle array was fabricated on silicon <100> wafer (p-type, resistivity 8-13 ohm-cm) coated with a monolayer consisting of polystyrene spheres with diameters of 520 nm. The monolayer was sputtered at oblique-angle incidence (70°) with a layer of Au with thickness of about 45 nm and subsequently annealed in a resistive furnace for 1 h at 700 °C.

Metal-assisted chemical etching was carried out at room temperature for 3 min in aqueous solution of HF (special safety precautions are necessary when handling this chemical even at low concentration) and H₂O₂ with concentration of 5% and 0.6%, respectively. After etching, the sample was rinsed in deionised water and dried under nitrogen stream. The gold nanoparticles were later removed by immersing the sample for 10 min in concentrated solution of I₂/KI.

For dry etching, the silicon substrate with the PtNP array prepared as described above (but with platinum) was loaded in an inductively coupled plasma (ICP) reactive ion etching system (Oxford Instruments, Plasmalab System 100, Yatton, UK). Sulfur hexafluoride (SF₆) and octafluorocyclobutane (C₄F₈) plasmas were used as etchants. The gas flow rates for SF₆ and C₄F₈ were 12 sccm and 27 sccm, respectively. During etching (2 min), the substrate was mechanically clamped and cooled (10 °C) by a backside flow of helium (10 sccm).

The samples were imaged using an FEI Quanta 400F scanning electron microscope (FEI Europe, Eindhoven) operating at an accelerating voltage of 10-15 KV and equipped with an Everhardt-Thornley SE detector.

3. Results and Discussion

The process reliably yielded particles arranged in a hexagonal array, often surrounded by small “satellite” NPs. The bottom-left SEM image in Fig.2a shows a typical array formed from an Au layer sputtered at normal incidence.

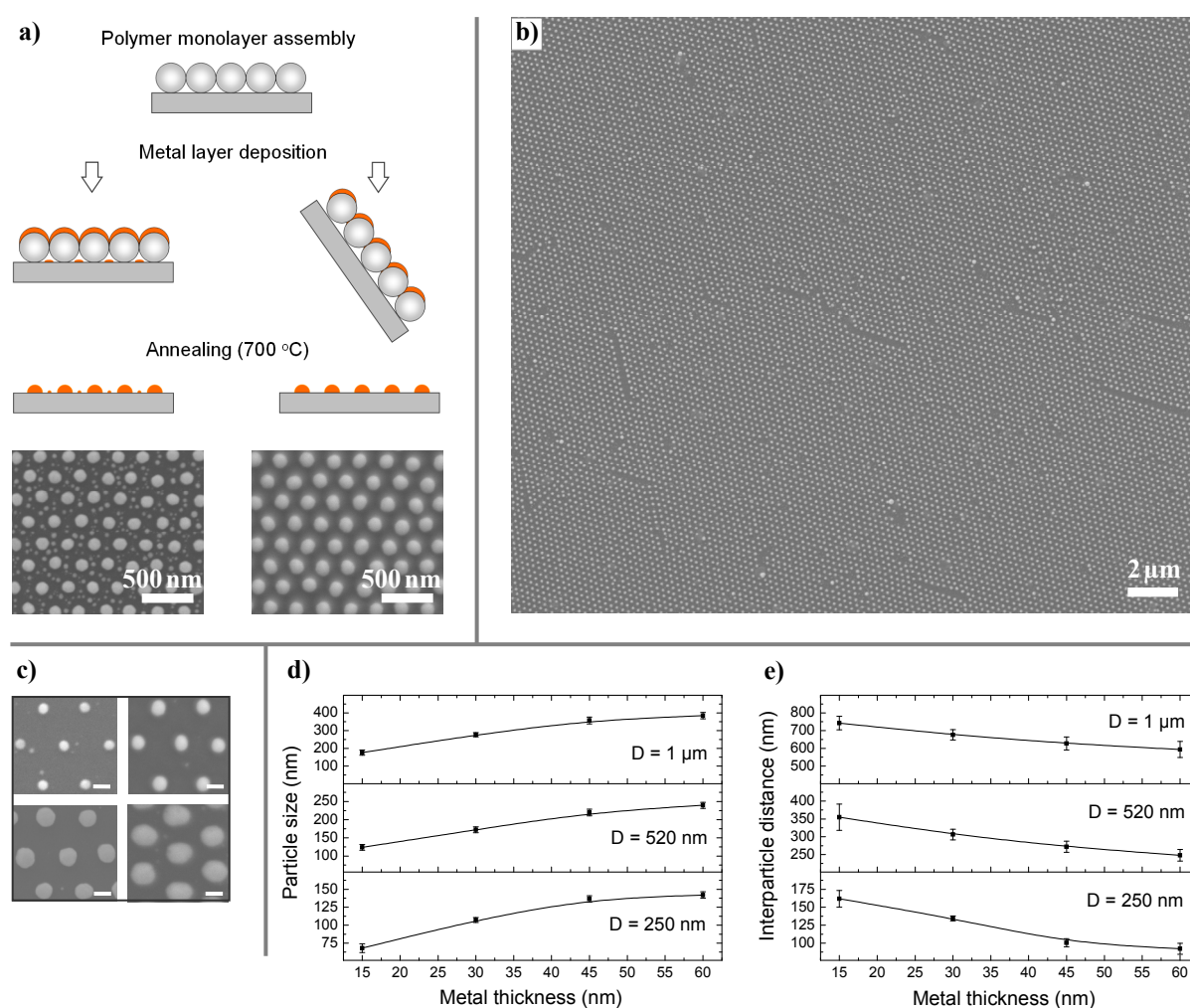


Figure 2. Process overview and metal array characterization. (a) Noble metal layer deposited at normal incidence (left) or at oblique incidence (right) at an angle between the sputtering beam direction and substrate normal in the range of 45° to 70° . SEM micrographs showing typical metal NP array formed in each particular case. (b) Example of large-area gold NP array. (c) Electron micrographs of AuNP arrays with area fraction occupied by the particles in the range of 7 – 38 % depending on initial metal layer thickness. Scale bar is 100 nm. (d) Influence of polystyrene sphere diameter (250 nm, 520 nm and 1 μm) and Au layer thickness (15 nm - 60 nm) on NP size and (e) on interparticle distance (gap). Each point indicates the mean and standard deviation estimated for NP size and interparticle distance, respectively.

The primary array originates from the metal layer deposited on top of each sphere while the satellite particles result from metal deposited in the interstices. The long-range order of the original polymer monolayer is well-preserved (Fig.2b). The number of satellites and their size can be significantly reduced by tilting the sample during sputtering, so that less metal is deposited through interstices as seen in the bottom-right SEM image of Figure 2a.

The annealing works equally well in a furnace or with an ethanol flame, with the latter having the advantage of speed. Thermal decomposition of metal-coated PS monolayers was achieved in less than two minutes when the front side or the back side of the samples were exposed to an ethanol flame (Fig. S2). The size of the resulting NPs and the gap between them depended both on the diameters of the spheres and the thickness of the metal film (Fig. 2 c-e). Figure 2d shows the dependence of resulting gold particle sizes on the thickness of Au layer deposited onto polystyrene spheres. The interparticle distance (i.e. the gap between particles) dependence on thickness is also shown (Fig. 2e). Polystyrene spheres with diameters ranging between 110 nm and 1 μm were found to yield metal particle arrays with narrow size distributions both on silicon (Fig. 3 a-d) and other substrate types such as fused silica and sapphire (Fig. S2 a,d).

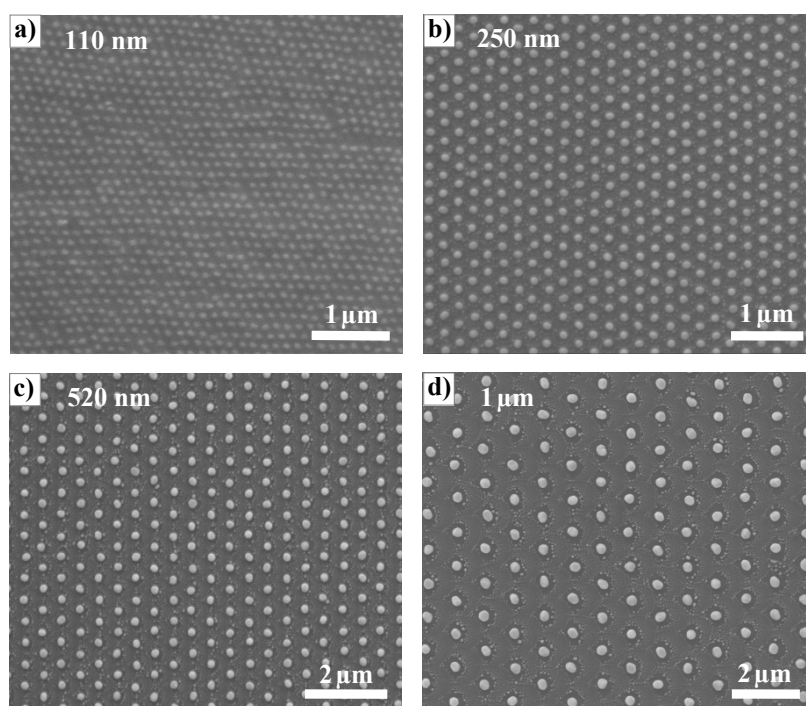


Figure 3. SEM micrographs of metal arrays fabricated on silicon from monolayers of polystyrene spheres of different diameters: (a) 110 nm, (b) 250 nm, (c) 520 nm and (d) 1 μm , sputtered with Au at 45° incidence and annealed at 700 °C for 1 h.

In the method used here, particle size and interparticle distance can be adjusted via the thickness of the metallic coating and the sphere diameter, respectively. As the volume of metal deposited on the top part of each individual sphere correlates to the volume of the resulting metal particle, we can estimate the final size of the metal particles based on the thickness of the initial metal layer. We found that the area fraction occupied by the particles can be tuned in the range of 7 – 40 %. When the metal layer was too thick, particles coalesced (Fig. S3). Temperatures in the range of 500-700 °C were used with fused silica, silicon, and sapphire substrates. Annealing at temperatures exceeding 700 °C for longer time (>2h) favoured the formation of faceted nanoparticles. Figure S4 shows a closer view of such an array. The particles appear to have a quasispherical shape. A tilted SEM image in Fig. S5 reveals the quasispherical shape of the resulting particles. Figure S6 highlights the difference between stochastic particles generated by dewetting^[27] of the initial metal layer deposited on bare substrate (left side of the image) and the ordered particles produced from thermal decomposition of the metal-coated polystyrene monolayer. Glass, mica or oxide substrates are expected to work equally well with this method.

Unwanted satellites can also be removed by wet etching. Figure S7a shows a metal array on silicon obtained by sputtering the Au layer at normal incidence and subsequent annealing. An etching solution of aqueous I₂/KI removed the satellite NPs and decreased the NPs size of the primary array (Fig. S7b).

The fabrication process is surprisingly robust against defects in the PS monolayers. Convective assembly sometimes produces double layers or even multiple layers. Remarkably, the resulting metal arrays are not critically affected by the presence of these extra layers as long as they retain long-range order, which is often the case. Both the metal deposited on monolayers and on the top layer of multilayers is converted into metal particle arrays. The lateral position of metal particles on the substrate always reflects the original position of the topmost polymer particles (Fig. S8).

The self-assembled multilayers occasionally exhibit quadratic packing of the topmost layer, which is faithfully transferred into the metal array, thus disrupting the hexagonal long range order.

The method is not limited to flat substrates: 3D objects can also be patterned. Figure 4 shows a glass tube (diameter = 180 μm) patterned with an array of AuNPs after decomposition of the polystyrene monolayer deposited by dip-coating.

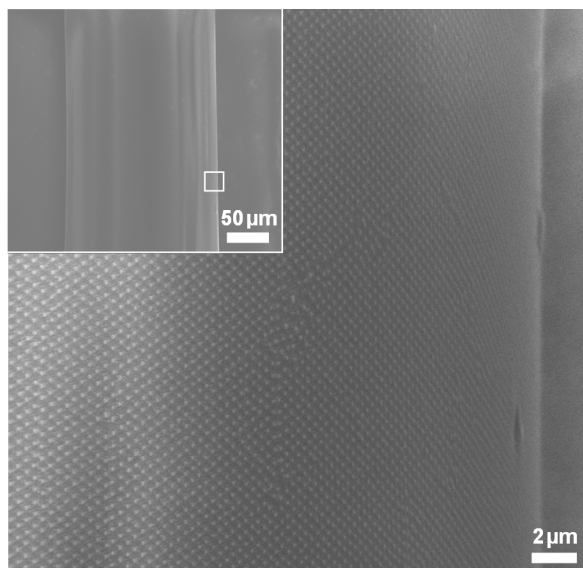


Figure 4. Metal NP array produced on the outer surface of a glass tube with a diameter of 180 μm by decomposition of Au-coated PS spheres ($D = 520 \text{ nm}$) using an ethanol flame. Inset: low magnification view showing a selected area of the tube's surface.

We show two examples of silicon nanostructuring based on metal NP arrays formed with the method presented in this report. Ordered noble metal NPs can serve as catalysts for metal-assisted chemical etching (MACE) in an aqueous solution of HF and H_2O_2 . Figure 5a reveals the holes array left behind after removing the AuNPs. Further parameter optimisation may be required to improve the directionality and morphology of the holes.

In the second example, a silicon wafer was nanostructured by dry etching masked by an array of PtNPs produced with our method. Figure 5b shows an SEM micrograph of the sample surface with a forest of silicon pillars, $\sim 200 \text{ nm}$ in diameter and $\sim 280 \text{ nm}$ in height with the platinum NPs located atop the pillars.

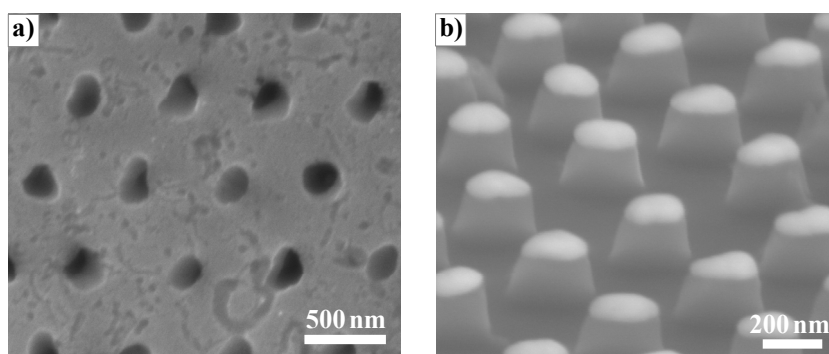


Figure 5. SEM micrographs of silicon nanostructures achieved using NP arrays. (a) Array of holes in silicon after metal-assisted chemical etching in aqueous solution of HF and H_2O_2 using the ordered AuNPs as catalysts. (b) Tilted SEM image showing silicon pillars fabricated by dry etching with processing gas mixture of $\text{SF}_6:\text{C}_4\text{F}_8$ using a PtNP array for nanomasking.

We analysed the decomposition process that is central to the formation of our arrays. Two polystyrene monolayers of the same particle type assembled on silicon substrates were annealed in a resistive furnace at a temperature of 200 °C for 20 min. One of the samples had a thin Au layer (~ 5 nm) deposited by sputtering at normal incidence, while the other sample was used as a reference. The temperature was chosen low enough to avoid complete decomposition of the polystyrene monolayers. The results suggest that the formation mechanism of the particle arrays depends on the metal layer's strength: while the uncoated monolayer melted and formed thin stripes of polystyrene (Fig. S9a), the gold-coated monolayer retained its geometry (Fig. S9b). Further annealing of the latter at elevated temperatures (700 °C) resulted in a metal array on the silicon surface, whereas the uncoated monolayer decomposed entirely at that temperature, leaving no residue behind (images not shown). The thermolysis of the polymer monolayer begins while the metal layer is still present to preserve its long-range order. As the temperature increases, the metal becomes mobile, minimises its surface energy and disperses into metal NP arrays. Samples annealed upside-down produced very similar results, proving that gravity does not play a significant role. Decomposition of larger metal-coated PS particles (3 μm and 15 μm) resulted in dewetting patterns instead of compact particles in the primary array (Fig. S10). Our findings indicate that the arrays form because the polystyrene particles decompose while the metal film slowly ripens into particles.

4. Conclusion

In summary, we reported a novel fabrication method for ordered arrays of metal nanoparticles that exploits the uniform arrangement of polymer beads deposited as close-packed monolayers. Large arrays (square cm) of noble metal (Au, Ag, Pt) nanoparticles were produced in a three-step process on silicon, fused silica and sapphire substrates, demonstrating the generality of this approach. Polystyrene spheres with diameters ranging between 110 nm and 1 μm were convectively assembled into crystalline monolayers, coated with metal and annealed in a resistive furnace or using an ethanol flame. The thermal decomposition of the polymer microspheres converted the metal layer into particles arranged in hexagonal arrays that preserved the order of the original monolayer. Both particle size and interparticle distance were adjusted via thickness of the metal coating and sphere diameter, respectively. This simple and reliable method yields dense metal NP arrays on a variety of substrates. The entire

metal is converted into particles, unlike in conventional lithography, where a significant fraction is lost in the process. We showed that the noble particle arrays produced with this method can be used for 3D nanostructuring of silicon surface on two distinct etching routes.

The highly versatile novel approach reported here can play an important role in development of advanced functional nanostructures.

Acknowledgements

We thank Susanne Selzer for her help with dry etching of silicon samples. Funding from the German Science Foundation (DFG) in the framework of priority program 1420, is gratefully acknowledged. Funding from the Australia-Germany Researcher Mobility Program is also acknowledged.

References

- [1] Zhang X, Zhao J, Whitney A V, Elam J W and Van Duyne R P 2006 Ultrastable Substrates for Surface-Enhanced Raman Spectroscopy Fabricated by Atomic Layer Deposition: Improved Anthrax Biomarker Detection *J. Am. Chem. Soc.* **128** 10304-09
- [2] Chen H L, Chuang S Y, Lin C H and Lin Y H 2007 Using colloidal lithography to fabricate and optimize sub-wavelength pyramidal and honeycomb structures in solar cells *Optics Express* **15** 14794-803
- [3] Mokkaapati S, Beck F J, Polman A and Catchpole K R 2009 Designing periodic arrays of metal nanoparticles for light-trapping applications in solar cells *Appl. Phys. Lett.* **95** 053115
- [4] Nakayama K, Tanabe K, and Atwater H A 2008 Plasmonic nanoparticle enhanced light absorption in GaAs solar cells *Appl. Phys. Lett.* **93** 121904
- [5] Papadopoulos C, Boogaard R S V D, Clutterbuck S, Lindsay G M and Winnitoy S R 2007 Large-area ordered C60 nanoparticle arrays *Nanotechnology* **18** 245306
- [6] Wood M A 2007 Colloidal lithography and current fabrication techniques producing in-plane nanotopography for biological applications *J. R. Soc. Interface* **4** 1-17
- [7] Shipway A N, Katz E and Willner I 2000 Nanoparticle Arrays on Surfaces for Electronic, Optical, and Sensor Applications *ChemPhysChem.* **1** 18-52
- [8] Contreras A M, Grunes J, Yan X M, Liddle A and Somorjai G A 2006 Fabrication of 2-dimensional platinum nanocatalyst arrays by electron beam lithography: ethylene hydrogenation and CO-poisoning reaction studies *Topics in Catalysis* **39** 123
- [9] Henzie J, Lee J, Lee M H, Hasan W and Odom T W 2009 Nanofabrication of Plasmonic Structures *Annu. Rev. Phys. Chem.* **60** 147-65
- [10] Vogel N, Weiss C K and Landfester K 2012 From soft to hard: the generation of functional and complex colloidal monolayers for nanolithography. *Soft Matter* **8** 4044-4061

- [11] Zhang J, Li Y, Zhang X and Yang B 2010 Colloidal Self-Assembly Meets Nanofabrication: From Two-Dimensional Colloidal Crystals to Nanostructure Arrays *Adv. Mater.* **22** 4249-4269
- [12] Murray E, Born P and Kraus T 2011 In *Generating Micro- and Nanopatterns on Polymeric Materials* (Eds: A del Campo, E Arzt), Wiley-VCH: Weinheim, Germany Ch. 9 pp 171-198
- [13] Ye Xiaozhou and Qi Limin 2011 Two-dimensionally patterned nanostructures based on monolayer colloidal crystals: Controllable fabrication, assembly, and applications *Nano Today* **6** 608-631
- [14] Plettl A, Enderle F, Saitner M, Manzke A, Pfahler C, Wiedemann S and Ziemann P 2009 Non-Close-Packed Crystals from Self-Assembled Polystyrene Spheres by Isotropic Plasma Etching: Adding Flexibility to Colloid Lithography *Adv. Funct. Mater.* **19** 3279-3284
- [15] Chih-Hung Sun, Wei-Lun Min and Peng Jiang 2008 Templated fabrication of sub-100 nm periodic nanostructures *Chem. Commun.* **27** 3163-3165
- [16] Tan B J Y, Sow C H, Koh T S, Chin K C, Wee A T S and Ong C K 2005 Fabrication of Size-Tunable Gold Nanoparticles Array with Nanosphere Lithography, Reactive Ion Etching, and Thermal Annealing *J. Phys. Chem. B* **109** 11100-11109
- [17] Sinitskii A, Neumeier S, Nelles J, Fischler M and Simon U 2007 Ordered arrays of silicon pillars with controlled height and aspect ratio *Nanotechnology* **18** 305307
- [18] Wei Li, Weiming Zhao and Ping Sun 2009 Fabrication of highly ordered metallic arrays and silicon pillars with controllable size using nanosphere lithography *Physica E* **41** 1600-1603
- [19] Cheung C L, Nikolić R J, Reinhardt C E and Wang T F 2006 Fabrication of nanopillars by nanosphere lithography *Nanotechnology* **17** 1339-1343
- [20] Asoh H, Oide A and Ono S 2006 Formation of microstructured silicon surfaces by electrochemical etching using colloidal crystal as mask *Electrochemistry Communications* **8** 1817-1820
- [21] Blackledge C W, Szarko J M, Dupont A, Chan G H, Read E L and Leone S R 2007 Zinc oxide nanorod growth on gold islands prepared by microsphere lithography on silicon and quartz *J. Nanosci Nanotechnol.* **7** 3336-3339
- [22] Huang Z P, Fang H and Zhu J 2007 Fabrication of Silicon Nanowire Arrays with Controlled Diameter, Length, and Density *Adv. Mater.* **19** 744-748
- [23] Hulteen J C, Treichel D A, Smith M T, Duval M L, Jensen T R and Van Duyne R. P. 1999 Nanosphere Lithography: Size-Tunable Silver Nanoparticle and Surface Cluster Arrays *J. Phys. Chem. B* **103** 3854-3863
- [24] Manzke A, Vogel N, Weiss C K, Ziener U, Plettl A, Landfester K and Ziemann, P. 2011 Arrays of size and distance controlled platinum nanoparticles fabricated by a colloidal method *Nanoscale* **8** 2523-2528
- [25] Karg M, Jaber S, Hellweg T and Mulvaney P 2011 Surface Plasmon Spectroscopy of Gold-Poly-N-isopropylacrylamide Core-Shell Particles *Langmuir* **27** 820-827

- [26] Vogel N, Ziener U, Manzke A, Plettl A, Ziemann P, Biskupek J, Weiss C K and Landfester K 2011 Platinum nanoparticles from size adjusted functional colloidal particles generated by a seeded emulsion polymerization process *Beilstein J. Nanotechnol.* **2** 459
- [27] Müller C M, Mornaghini F C F and Spolenak R 2008 Ordered arrays of faceted gold nanoparticles obtained by dewetting and nanosphere lithography *Nanotechnology* **19** 485306
- [28] Kempa K, Kimball B, Rybczynski J, Huang Z P, Wu P F, Steeves D, Sennett M, Giersig M, Rao D V G L N, Carnahan D L et al. 2003 Photonic Crystals Based on Periodic Arrays of Aligned Carbon Nanotubes *Nano Lett.* **3** 13-18
- [29] Prevo B G and Velev O D 2004 Controlled, Rapid Deposition of Structured Coatings from Micro- and Nanoparticle Suspensions *Langmuir* **20** 2099-2107
- [30] Malaquin L, Kraus T, Schmid H, Delamarche E and Wolf H 2007 Controlled particle placement through convective and capillary assembly *Langmuir* **23** 11513-11521
- [31] Born P, Blum S, Munoz A and Kraus T 2011 Role of the Meniscus Shape in Large-Area Convective Particle Assembly *Langmuir* **27** 8621-8633

Supplementary data

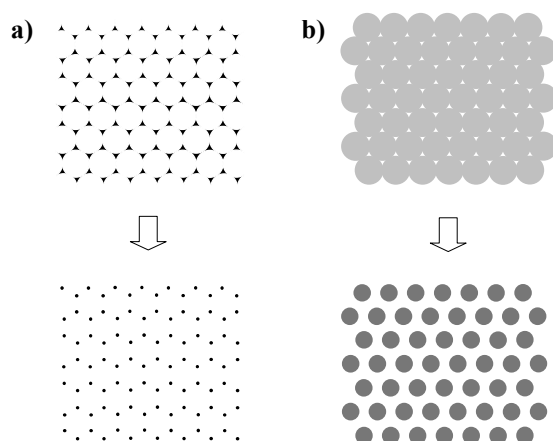


Figure S1. Schematic comparison of packing arrangement (a) Standard colloidal lithography using the polymer monolayer as a mask that is subsequently removed in organic solvent. The ordered quasi-triangular islands can be further converted into metal NPs via annealing (b) Our process in which thermal decomposition of metal-coated polymer monolayer yields metal NP array.

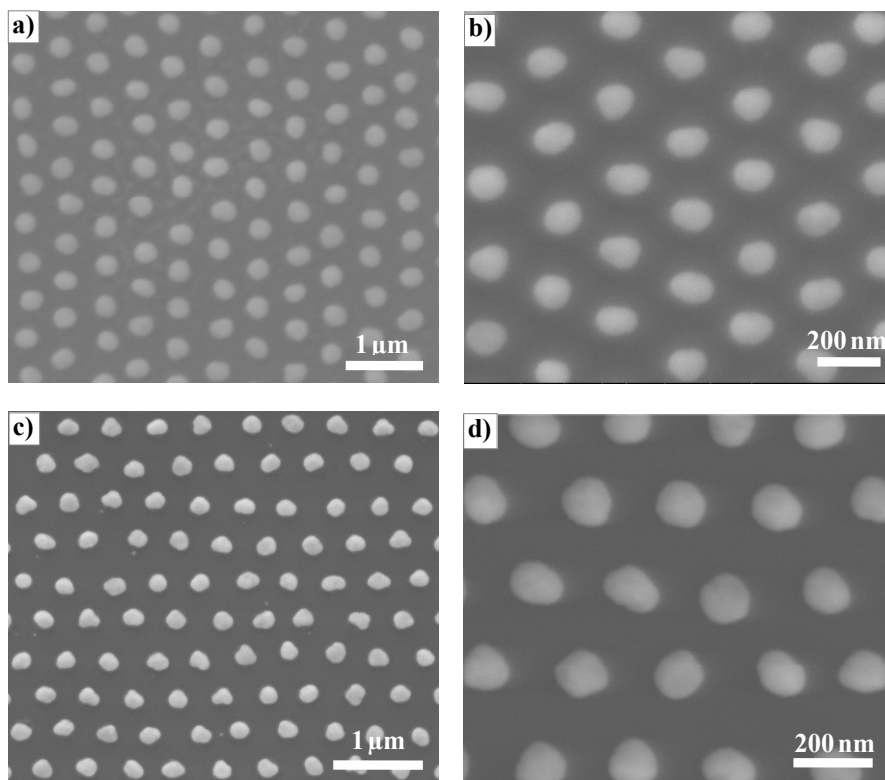


Figure S2. Examples of metal NP arrays achieved by flame annealing on different substrates. (a) PtNPs produced using the flame applied for 2 min directly to the metal-coated polystyrene monolayer assembled on fused silica and (b) on silicon substrate; (c) PtNPs generated by applying the flame for 2 min on the back side of silicon and (d) on single crystal Al_2O_3 substrate.

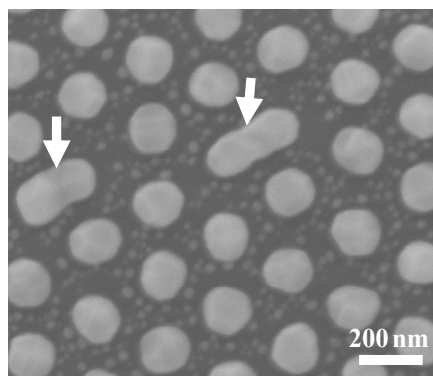


Figure S3. SEM micrograph showing particle coalescence when the initial metal layer is too thick. Polystyrene monolayer ($D = 250$ nm) assembled on silicon, sputtered with 70 nm Au layer and annealed at 700°C for 1h. The arrows indicate particles that coalesced during annealing.

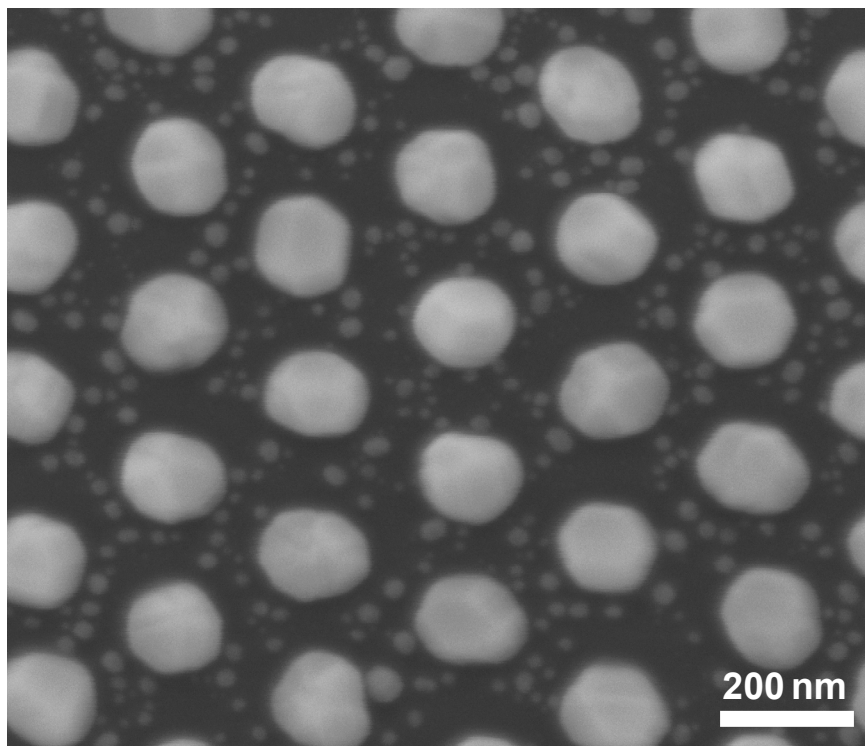


Figure S4. Close view SEM micrograph showing an array of faceted AuNP produced on silicon substrate by annealing at 700 °C for 2 h.

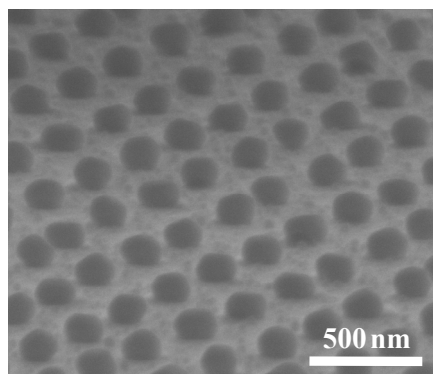


Figure S5. Tilted SEM micrograph showing the quasispherical shape of AuNPs

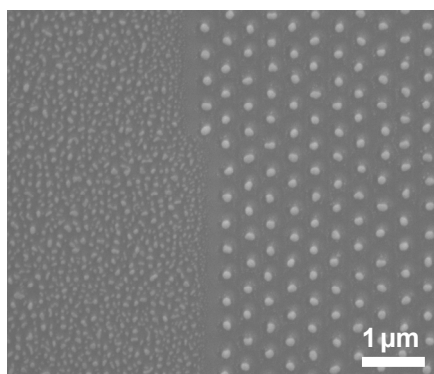


Figure S6. SEM micrograph showing the edge between stochastically arranged PtNPs (left side of the image), resulted from dewetting of Pt thin film deposited directly on silicon substrate near the area of close-packed PS monolayer, and the ordered PtNPs (right side) formed by decomposition of Pt coated PS monolayer.

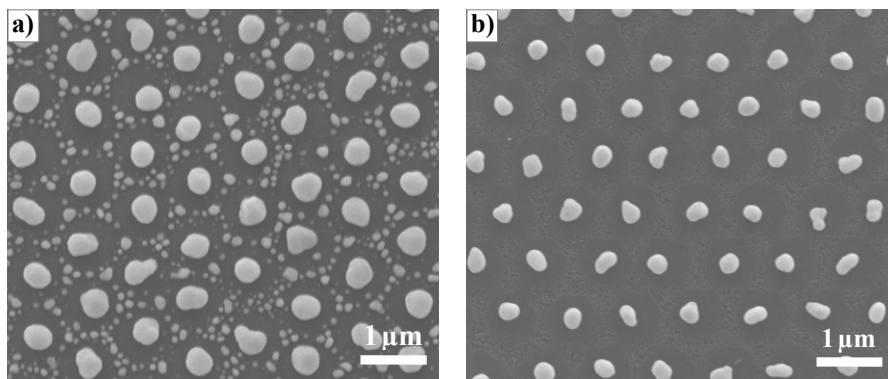


Figure S7. Wet etching of the secondary pattern (satellite NPs) (a) SEM image of an AuNP array fabricated on silicon by Au sputtering at normal incidence and subsequently annealing at 600 °C for 1h. (b) Image of the same sample after wet etching in aqueous I_2/KI solution for 10 min.

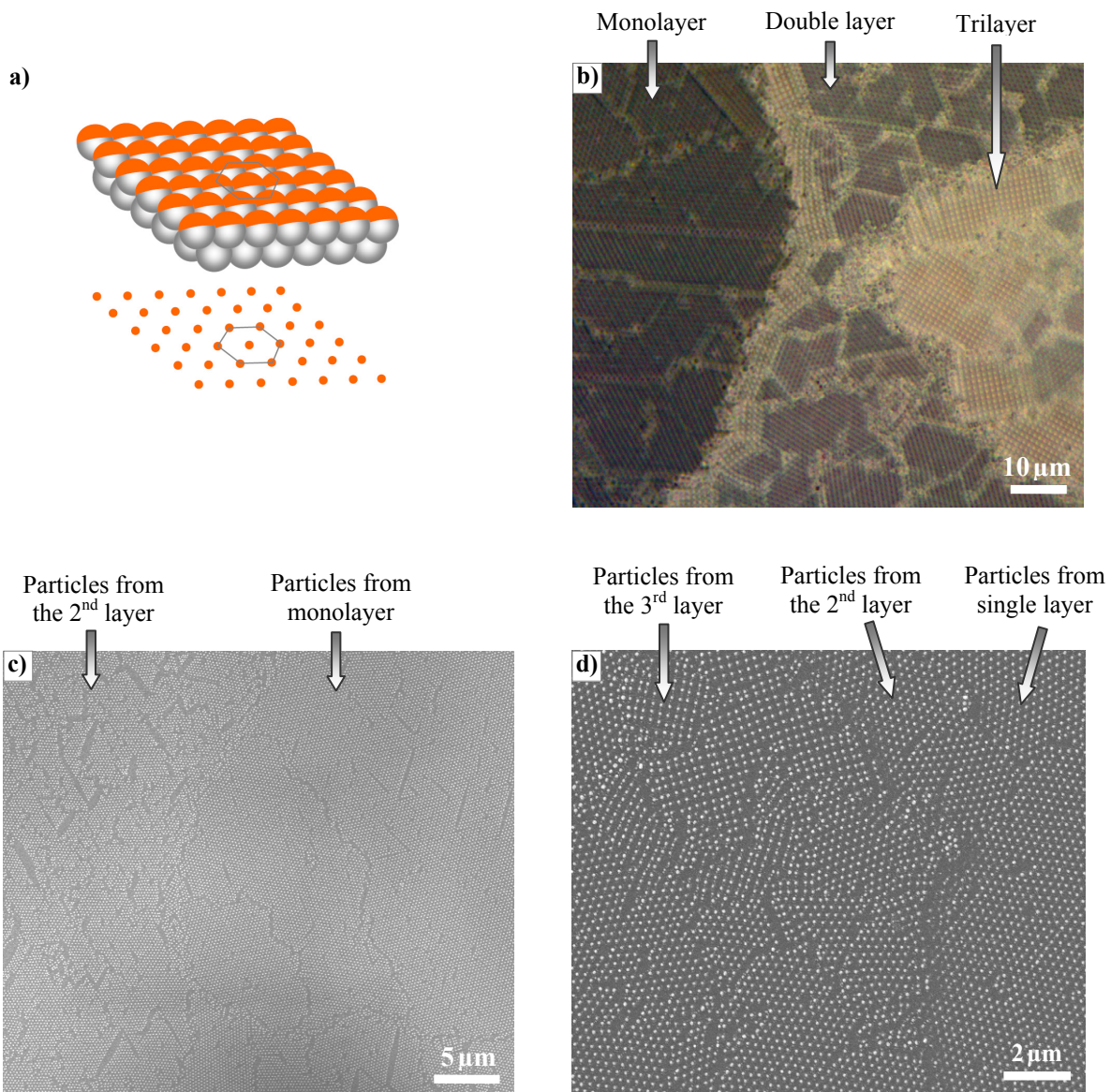


Figure S8. Two-dimensional NP array formed from metal-coated polymer multilayers. (a) Schematic view. (b) Optical microscopy image showing the formation of quadratic packing in PS multilayer. (c, d) SEM micrographs of NP array produced on silicon substrate by annealing of Au coated PS multilayers.

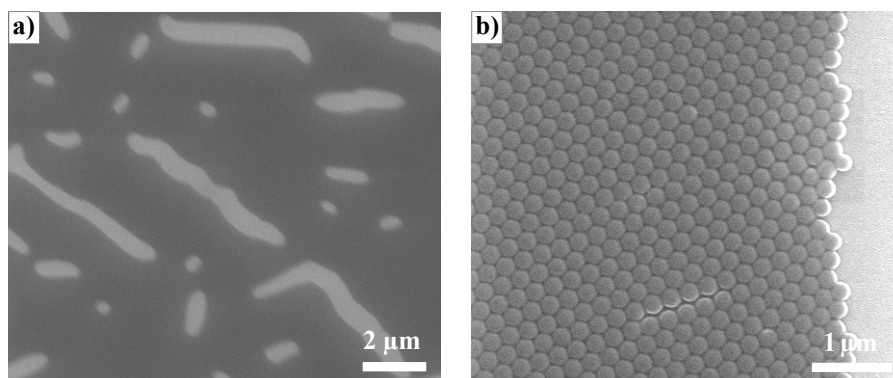


Figure S9. SEM micrographs of polystyrene ($D_{sp} = 250$ nm) monolayers under two distinct conditions: (a) without metal coating and (b) with a 5 nm thick Au layer, both after annealing at 200 °C for 20 min.

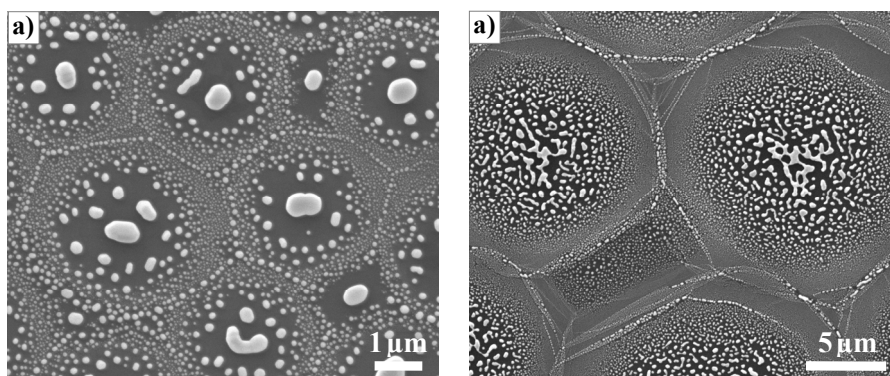


Figure S10. Dewetting patterns produced on silicon surface by annealing (700 °C, 2 h) of Au coated monolayers of PS particles with diameters of (a) 3 μm and (b) 15 μm

Each individual polymer sphere is loaded with a constant amount of metal in the form of fine grains. The PS decomposition process brings together these metal grains and promotes their melting into one bigger particle as temperature increases. The dewetting process on substrate surface occurs without losing the long range order of the initial close-packed PS layer, most likely because the same amount of metal is involved for each resulting particle. When polymer particles exceed a certain size however, due to lower surface-to-volume ratio it becomes increasingly hard for the fine metal grains to cluster together and form a bigger metal lump during decomposition process. In such instance, they disperse into molten polymer and during polymer decomposition they eventually coalesce into a random pattern by dewetting as shown in Fig. S10.